JACS
JOURNAL OF THE AMERICAN CHEMICAL SOCIETY

Article

pubs.acs.org/JACS

Long Coherence Times in Nuclear Spin-Free Vanadyl Qubits

Chung-Jui Yu,[†] Michael J. Graham,[†] Joseph M. Zadrozny,[†] Jens Niklas,[‡] Matthew D. Krzyaniak,[†,§] Michael R. Wasielewski,[†,§] Oleg G. Poluektov,[‡] and Danna E. Freedman*[,†]

[†]Department of Chemistry, Northwestern University, Evanston, Illinois 60208, United States

[‡]Chemical Sciences and Engineering Division, Argonne National Laboratory, Argonne, Illinois 60439, United States

[§]Argonne-Northwestern Solar Energy Research (ANSER) Center, Northwestern University, Evanston, Illinois 60208-3113, United States

Supporting Information

ABSTRACT: Quantum information processing (QIP) offers the potential to create new frontiers in fields ranging from quantum biology to cryptography. Two key figures of merit for electronic spin qubits, the smallest units of QIP, are the coherence time (T_2), the lifetime of the qubit, and the spin−lattice relaxation time (T_1), the thermally defined upper limit of T_2. To achieve QIP, processable qubits with long coherence times are required. Recent studies on $(Ph_4P\text{-}d_{20})_2[V(C_8S_8)_3]$, a vanadium-based qubit, demonstrate that millisecond T_2 times are achievable in transition metal complexes with nuclear spin-free environments. Applying these principles to vanadyl complexes offers a route to combine the previously established surface compatibility of the flatter vanadyl structures with a long T_2. Toward those ends, we investigated a series of four qubits, $(Ph_4P)_2[VO(C_8S_8)_2]$ (**1**), $(Ph_4P)_2[VO(\beta\text{-}C_3S_5)_2]$ (**2**), $(Ph_4P)_2[VO(\alpha\text{-}C_3S_5)_2]$ (**3**), and $(Ph_4P)_2[VO(C_3S_4O)_2]$ (**4**), by pulsed electron paramagnetic resonance (EPR) spectroscopy and compared the performance of these species with our recently reported set of vanadium tris(dithiolene) complexes. Crucially we demonstrate that solutions of **1**−**4** in SO_2, a uniquely polar nuclear spin-free solvent, reveal T_2 values of up to 152(6) μs, comparable to the best molecular qubit candidates. Upon transitioning to vanadyl species from the tris(dithiolene) analogues, we observe a remarkable order of magnitude increase in T_1, attributed to stronger solute−solvent interactions with the polar vanadium-oxo moiety. Simultaneously, we detect a small decrease in T_2 for the vanadyl analogues relative to the tris(dithiolene) complexes. We attribute this decrease to the absence of one nuclear spin-free ligand, which served to shield the vanadium centers against solvent nuclear spins. Our results highlight new design principles for long T_1 and T_2 times by demonstrating the efficacy of ligand-based tuning of solute−solvent interactions.

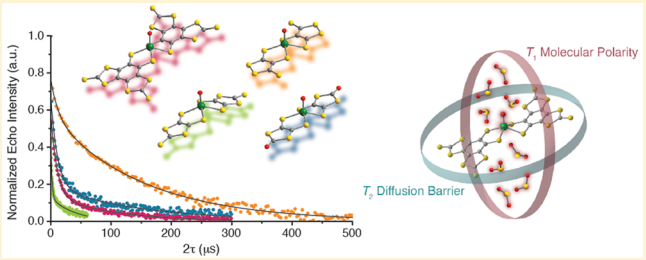

INTRODUCTION

Quantum information processing (QIP) is a powerful computational approach with the potential to revolutionize problem solving in fields ranging from cryptography to the modeling of quantum biological processes.[1−5] Implementation of QIP relies upon the manipulation of quantum bits, or qubits, that can be placed in a superposition of the binary states "0" and "1". Of the numerous approaches to creating qubits, one promising route employs pairs of electronic spin sublevels, M_S levels, in coordination complexes.[6−8] These molecular electronic spin-based qubits are advantageous for two crucial reasons: their capacity for facile addressing via pulsed electron paramagnetic resonance (EPR) techniques and significant chemical tunability via synthetic chemistry.[8,9] Further promise for electronic spin qubits resides in the prospect of coupling many such spin centers together within the same device.[7,10−15] Notably, employing transition metals as the source of electronic spin confers two additional dimensions of scalability beyond that of radical-based systems: the potential to incorporate a multitude of M_S levels, and therefore qubits, within the same complex, and the capability of creating hybrid electronic spin-nuclear spin-based quits through the use of hyperfine transitions on a single transition metal.[10,16−18]

The performance of a qubit system is described by two figures of merit: the coherence time (T_2), which is the time window of control for the qubit,[8] and the spin−lattice relaxation time (T_1), which serves as an upper limit to T_2 and the inverse of which ($1/T_1$) determines the qubit operating speed.[19,20] The primary challenge in the practical implementation of electronic spin-based qubits is slowing the collapse of the superposition state, a process known as decoherence or dephasing.[7,11] The time scale of decoherence is parametrized by T_2.[11] Enabling the rational synthesis of qubits relies upon creating specific design principles that allow chemists to rationally dial-in T_1 and T_2 values via chemical modification. While there are several powerful studies on qubit design, including our own, there remain many parameters to be investigated. Few studies have assessed the generality of qubit design principles discovered thus far, necessitating significant

Received: August 12, 2016
Published: October 31, 2016

DOI: 10.1021/jacs.6b08467
J. Am. Chem. Soc. 2016, 138, 14678−14685

further work to reveal universal design principles.[21−28] The absence of synthetic insight lies at the heart of the challenge of constructing viable molecular qubits.

Fundamental investigations of design principles for qubits are optimally performed on $S = {}^1/_2$ complexes, such as those of vanadium(IV), where there are a minimum number of convoluting variables. Further, employing vanadium as a qubit enables us to draw upon on the wealth of knowledge obtained via investigations of biological systems.[29−31] Indeed, recent studies revealed enormous promise for these species as electron spin-based qubits.[17,22,24,26,28,32−34] Of specific relevance to the studies described herein, one such complex, $[V(C_8S_8)_3]^{2-}$, exhibits a coherence time of 0.7 ms, unprecedented for molecular systems.[17,32] This result rivals the performance of current state-of-the-art solid state qubits,[35−38] and establishes the viability of coordination complexes as potential materials for QIP.

Demonstration of millisecond coherence times in molecular qubits propels the field forward toward preparing molecules amenable for device fabrication. Yet, as a nearly spherical molecule, $[V(C_8S_8)_3]^{2-}$ is ill-suited to this application. Progressing in that direction necessitates an additional design criterion, molecules that are compliant with deposition on surfaces. Note that these molecules still require long coherence times, analogous to those observed in $[V(C_8S_8)_3]^{2-}$.[11] One class of vanadium-based qubits that can potentially satisfy these criteria is square-pyramidal vanadyl(IV) complexes. Indeed, previous elegant research demonstrated the confluence of room-temperature quantum coherence and surface compatibility in these complexes.[22,33]

Marrying the surface compatibility of vanadyl(IV) complexes with the nuclear spin-free ligand field of $[V(C_8S_8)_3]^{2-}$ offers a pathway to create long-lived surface-compatible qubits. However, achieving this goal first requires establishing design principles governing T_1 and T_2 in vanadyl bis(dithiolene) qubits. We sought to both determine whether vanadyl-based qubits can display comparable times to vanadium tris(dithiolene) (hereafter notated as VS_6) qubits, and to determine the influence of ligand design on T_1 and T_2 in these species. For the first aim, we focused on creating an environment that simulates the nuclear spin-free environment of a future device.[11] The potential obscuring effect of large numbers of nuclear spins on subtle differences between complexes provides further impetus for removing nuclear spins from both the ligands and solvent. However, previous studies on VS_6 and vanadyl complexes largely employed nuclear spin-bearing solvents, as the only nuclear spin-free solvent that is a liquid under standard conditions is carbon disulfide (CS_2), which is highly nonpolar.[22,24,32,34] This low polarity results in extremely low solubility for most charged molecular qubits. In order to circumvent this restriction, we investigated unconventional nuclear spin-free solvents and discovered significant promise in the polar solvent sulfur dioxide.[39] Note that although SO_2 is a gas under standard conditions, it readily liquefies at −10 °C. While SO_2 is not a glassing solvent, and can therefore engender aggregation (and hence, additional decoherence processes) of the solute, it nevertheless provides a nuclear spin-free matrix with which to study charged qubit complexes.

Creating design principles for surface-compatible vanadyl species relative to VS_6 species appears, upon initial inspection, to be a trivial modification. Yet there are two significant differences between the classes of compounds. The first relates to the structural change moving from an approximate octahedral geometry to a square pyramidal geometry. This causes spin-containing solvent nuclei to occupy different positions relative to the vanadium center in the two molecule types—an important consideration as environmental nuclear spins are frequently a main contributor to decoherence.[19,25,32,40] The two configurations of the metal ion also alter the strength of the molecule's vibrational coupling with the surrounding solvent molecules, which can affect T_1. The second dramatic change is in the orbital containing the unpaired electron; in vanadyl complexes it is predominately $d_{x^2-y^2}$ in character, whereas in VS_6 complexes the orbital is predominately d_{z^2} in character.[41−45] This change modifies the extent of the electron delocalization from the metal center, potentially increasing interactions of the unpaired electron with the local environment, and therefore affecting decoherence and spin−lattice relaxation.[46] In the expansive EPR literature on both vanadyl and VS_6 complexes,[42,47−53] there is a sole, recent investigation on the effect of substituting a vanadyl complex for the analogous VS_6 complex on T_2 and T_1.[28] However, the scope of this study was limited to the examination of a single pair of complexes in the solid state and at relatively high concentrations. To rigorously develop future design principles and establish whether long coherence times in vanadium-based qubits are generalizable, a more expansive study probing a series of complexes in modular, solution-phase systems is required. Importantly, our utilization of the unique nuclear spin-free solvent SO_2 enables us to deconvolute the effect of local variables from the external matrix environment.

In order to address the dearth of design principles underlying vanadyl qubits and studies of processable qubits in spin-free environments, we report herein the synthesis and characterization of a series of vanadyl complexes with nuclear spin-free ligands in both spin-bearing solvents and SO_2. Taken together with our group's previous investigation of an analogous series of four VS_6 complexes, this set of complexes offers insight into design criteria for future device-ready qubits.

RESULTS AND DISCUSSION

To enable the clearest study, vanadyl complexes $(Ph_4P)_2[VO(C_8S_8)_2]$ (**1**), $(Ph_4P)_2[VO(\beta\text{-}C_3S_5)_2]$ (**2**), $(Ph_4P)_2[VO(\alpha\text{-}C_3S_5)_2]$ (**3**), and $(Ph_4P)_2[VO(C_3S_4O)_2]$ (**4**) were synthesized with the same set of nuclear spin-free carbon−sulfide ligands previously employed in the analogous four tris(dithiolene) complexes $(Ph_4P)_2[V(C_8S_8)_3]$ (**1′**), $(Ph_4P)_2[V(\beta\text{-}C_3S_5)_3]$ (**2′**), $(Ph_4P)_2[V(\alpha\text{-}C_3S_5)_3]$ (**3′**), and $(Ph_4P)_2[V(C_3S_4O)_3]$ (**4′**) (Figure 1). All four vanadyl complexes possess a square pyramidal geometry around the vanadium center. Within the series, V═O bond lengths range from 1.599(4) to 1.605(3) Å, and V—S bond lengths range from 2.306(2) to 2.395(2) Å, comparable to those seen in other vanadyl complexes with thiolato sulfur donors.[44,47,48,54,55]

We first sought to investigate differences in the extent of electron delocalization between the two series, as this may have important implications for qubit performance. To measure the hyperfine coupling across the vanadyl series, and thereby probe the extent of electron delocalization away from the vanadium center, we performed continuous-wave (CW) EPR spectroscopy at X-band frequency (9.68 GHz) on 0.5 mM solutions of **1**−**4** (see Figure S1). The impact of differing nuclear spin environments was explored by measuring **1**−**4** in both 1:1 dimethylformamide:toluene (DMF:Tol) and 1:1 DMF-d_7:Tol-d_8. CW spectra for the complexes exhibit eight transitions

DOI: 10.1021/jacs.6b08467
J. Am. Chem. Soc. 2016, 138, 14678−14685

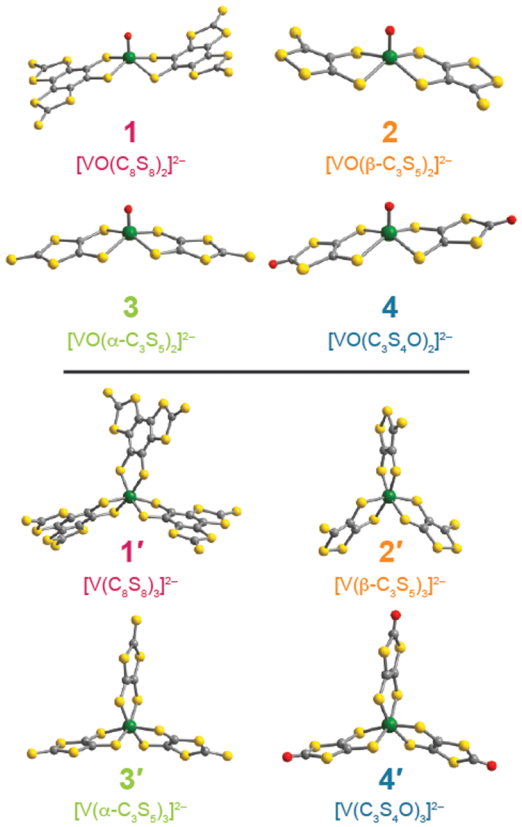

Figure 1. Molecular structures of the vanadyl complexes **1**−**4** (top half) and the analogous VS_6 complexes **1′**−**4′** (bottom half) synthesized in a previous report.[32] Green, yellow, red, and gray represent vanadium, sulfur, oxygen, and carbon, respectively.

corresponding to the $S = {}^1/_2$ state coupling with the $I = {}^7/_2$ ^{51}V nucleus. Easyspin[56] was used to fit the spectra to quantify axial hyperfine coupling ($\boldsymbol{A}$) and g parameters employing the Hamiltonian $\hat{H} = g\mu_B\boldsymbol{HS} - g_N\mu_N\boldsymbol{HI} + \boldsymbol{IAS}$, where g is the axial g-tensor, μ_B is the Bohr magneton, $\boldsymbol{H}$ is the magnetic field, $\boldsymbol{S}$ is the electronic spin, g_N is the nuclear g-tensor, μ_N is the nuclear magneton, $\boldsymbol{I}$ is the nuclear spin, and $\boldsymbol{A}$ is the axial hyperfine coupling tensor. Modeling the spectra as axial systems yielded $g_\parallel$ = 1.971−1.976, $g_\perp$ = 1.989−1.990, $A_\parallel$ = 411−418 MHz, and $A_\perp$ = 131−132 MHz (see Tables S5 and S6); these values are in accord with those of other vanadyl bis(dithiolene) complexes.[28,49,50,53] Values of g and A were identical in the protiated and deuterated solvent matrices, indicating no significant change in molecular geometry as a function of solvent.

Averaged hyperfine tensor values for the vanadyl series of **1**−**4** fell within the narrow range of $\langle|A|\rangle$ = 224−227 MHz. Values for the previous series of VS_6 compounds, which were fit assuming only positive signs of A_x, A_y, and A_z, showed complexes **2′**−**4′** in a similarly narrow range, $\langle|A|\rangle$ = 235−248 MHz, while the low value of **1′** ($\langle|A|\rangle$ = 192 MHz) served as an outlier.[32] The differences in $\langle|A|\rangle$ suggest that the unpaired electron in **1**−**4** may be more delocalized from the vanadium center than in **2′**−**4′**, but less so than in **1′**. Conclusions on the amount of delocalization between **1**−**4** and **1′**−**4′** are complicated by the differing geometries, but the significant difference in $\langle|A|\rangle$ between **1′** and **2′**−**4′** allows for a direct comparison within the VS_6 series. Therefore, any differences in properties arising from different delocalization between **1**−**4** and **1′**−**4′** should also manifest between **1′** and **2′**−**4′**.

Our initial goal was to establish whether the same design principle of a nuclear spin-free ligand field is viable within vanadyl complexes. Here, the absence of a large ligand shielding the metal center from solvent interactions, coupled with the increased electron delocalization into the ligand field, led us to ask whether the coherence times of **1**−**4** would be comparable to those observed in VS_6 complexes. Therefore, we endeavored to measure **1**−**4** in a nuclear spin-free solvent. Predictably, our attempts to solubilize the vanadyl complexes in CS_2 were unsuccessful, which we attribute to the complexes' 2− charge and the low polarity of CS_2. Indeed, these challenges are likely the reason so few molecular qubit candidates are measured in this convenient solvent. We circumvented the solubility problem by utilizing SO_2, a polar nuclear spin-free molecule, as a solvent, the same solvent employed in previous study of ours.[39] To the best of our knowledge, this is the only previous report of the use of SO_2 as a solvent for candidate qubits.

Hahn echo experiments performed on the central resonance of 0.13 mM solutions of the complexes in SO_2 at 10 K yielded coherence times, extracted from the long component of the biexponential fit, of 40(1)−152(6) μs, with the highest values observed in **2** (151(2) μs) and **4** (152(6) μs) (Figure 2). These coherence times are among the longest observed in molecular qubits, eclipsed only by $(Ph_4P\text{-}d_{20})_2[V(C_8S_8)_3]$ in CS_2.[32] Note that the biexponential decay character suggests the presence of two distinct decoherence processes. Here, we attribute the faster relaxation process to electron spin-electron spin coupling caused by aggregation of the complex or counterions, and the slower process to nuclear spin diffusion. Aggregation induces decoherence by increasing the proximity of the complexes, and hence the electronic spins, to each other, allowing neighboring spins to mutually interfere. Frozen SO_2 is not a glass, and therefore readily provides opportunities for aggregation along the numerous crystalline grain boundaries of the frozen solvent matrix.[32] While the non-glassing behavior certainly is not ideal, the T_2 values extracted from the slow relaxation process nevertheless provide a measure of the intrinsic coherence times of **1**−**4** in nuclear spin-free environments. Even when the fast process for each of the species is neglected, the T_2 values of the vanadyl complexes at 10 K remain several orders of magnitude lower than T_1 (Table S14). We attribute the observation that T_2 is not T_1-limited to the nuclear spins of the non-deuterated Ph_4P^+ cations, which remain a source of protons in the otherwise proton-free environment. Note, Ph_4P^+ also contains ^{31}P which provides a second source of nuclear spin. Despite the promotion of decoherence by both proximal nuclear spins and complex aggregation, T_2 values for these systems are nearly two orders of magnitude longer than those observed for all previous measurements of molecular vanadyl qubits. This measurement in SO_2 enables us to fully isolate these molecules from adjacent nuclear spins, thereby enabling the realization of coherence times that are substantially longer than those observed in the solid state.[28] These results demonstrate that extraordinary coherence times are attainable in vanadyl complexes in SO_2 and the utility of SO_2 as a polar, nuclear spin-free solvent for future studies—both our own and those of the community at large.

In light of the results above, we performed nutation experiments to determine whether **1**−**4** can be placed into any arbitrary superposition of states. Demonstration of this capability establishes a candidate molecule's viability as a qubit. Nutation experiments can also quantify the gate time for the

DOI: 10.1021/jacs.6b08467
J. Am. Chem. Soc. 2016, 138, 14678−14685

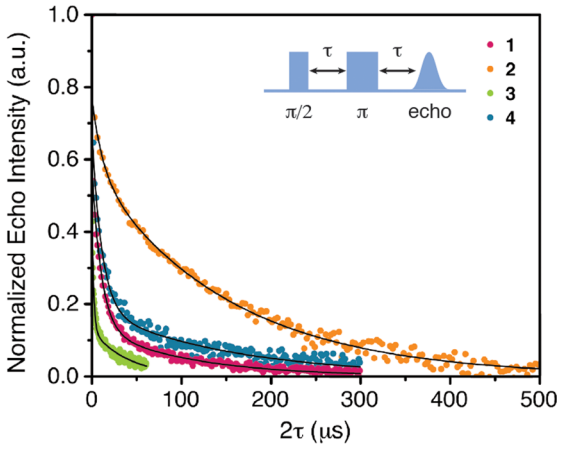

Figure 2. Normalized Hahn echo decay curves of **1**−**4** in SO_2 at 10 K. The black lines correspond to biexponential fits of the data. The pulse sequence of the Hahn echo experiment is shown.

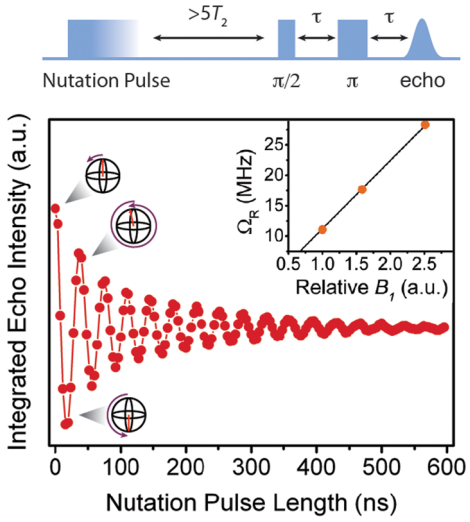

Figure 3. Nutation experiment performed on **1** in 1:1 DMF-d_7:Tol-d_8 showing Rabi oscillations that demonstrate the capability of the complex to be placed in any arbitrary superposition between the $M_S = -^1/_2$ and $M_S = +^1/_2$ spin states. The spin orientation as a function of pulse length is depicted alongside the nutation data. A diagram of the pulse sequence used for nutation measurements is shown above. A linear dependence is observed between the Rabi frequency and the pulsed field strength.

simplest logic gate: a NOT gate. Toward those ends, a variable length microwave pulse (a nutation pulse) was applied to 0.5 mM solutions of the complexes in both 1:1 DMF:Tol and 1:1 DMF-d_7:Tol-d_8 at the central resonance, followed by a two-pulse sequence to generate an echo that detects the turning angle. Because the applied magnetic field quantizes the alignment of the spin into two discrete states, denoted down ($M_S = -^1/_2$) and up ($M_S = +^1/_2$), any spin alignment that deviates from one of these states constitutes a superposition of the two states. A viable qubit will display a continuous decaying oscillation (Rabi oscillation) of echo intensity as the qubit cycles through all possible superposition states.[57,58] We observe in our system of vanadyl complexes this decaying oscillation as the nutation pulse length increases (Figure 3, see also Figures S7 and S8). Note that nuclear spins and cavity effects[59] can also contribute oscillations to the echo intensity. These contributions necessitate measuring the Rabi frequency at multiple pulsed field strengths, as the frequency of true nutations is linearly proportional to the pulsed microwave field strength (B_1) for true Rabi oscillations. The unique Rabi frequency extracted from these measurements has also been used in quantum sensing applications as a mechanism of probing the local environment.[60] Fourier transforms of the Rabi oscillations for **1**−**4** at different pulsed fields in 1:1 DMF:Tol and 1:1 DMF-d_7:Tol-d_8 yield Rabi frequencies of 9.8−29.8 MHz. Within the series of compounds, spin-flip times, corresponding to NOT gates, ranged from 17 to 53 ns. Crucially, a linear relationship is present between the Rabi frequency and B_1, which demonstrates these oscillations can be attributed to quantum control, not nuclear spins or cavity effects (Figure 3; see also Figure S9). These data confirm our candidate qubits can be placed into any arbitrary superposition, establishing them as qubits.

With a demonstration that these species display coherence times suitable for implementation and Rabi oscillations, we further sought to investigate the design principles underlying vanadyl qubits. Enabling the directed synthesis of further vanadyl qubits necessitates creating design principles beyond that of nuclear spin-free ligand environments. Toward that end, we investigated the spin−lattice relaxation times (T_1) of **1**−**4** via pulsed EPR. Spin−lattice relaxation is the phonon-mediated electronic spin transition from the excited to ground Zeeman energy levels. The degree to which phonons contribute to spin−lattice relaxation depends on a number of factors, including vibrational modes of the molecule and its local environment, the presence or absence of low-lying excited states, and the spin−orbit coupling of the unpaired electron.[19] T_1 therefore serves as a sensitive probe of both the molecule's intrinsic properties and its interaction with the local environment.

Acquisition of T_1 data first proceeded by inversion recovery experiments on 0.5 mM solutions of **1**−**4** in 1:1 DMF:Tol from 10 to 140 K. All experiments were performed at the highest intensity central resonance in the EPR spectrum. At 10 K, T_1 for **1**−**4** ranges from 16.29(8) to 23.8(2) ms and rapidly decreases with increasing temperature, ultimately reaching 6.62(5)−11.38(8) μs at 140 K. Values of $1/T_1$ for **1**−**4** are depicted alongside those of **1′**−**4′** in Figure 4 (see also Figure S2). Interestingly, we found the magnitudes of the T_1 values for **1**−**4** to be one-half to one order of magnitude larger than those observed in **1′**−**4′** across the entire temperature range measured. This disparity is similar to that observed by Sessoli and co-workers in their recent comparative study.[28] Within the vanadyl series, the T_1 values are nearly identical, demonstrating that different ligands within the series do not appreciably impact T_1. This mirrors the previous measurements on **1′**−**4′**, which demonstrated a similar lack of T_1 ligand dependence. In addition, very similar T_1 values were obtained with **1**−**4** in DMF-d_7:Tol-d_8, indicating that the change in lattice phonon modes caused by deuteration has a negligible effect on spin−lattice relaxation, as previously noted.[61]

Elucidating the key molecular differences in **1**−**4** and **1′**−**4′** that result in this dramatic change in T_1 is critical to understanding how to tune this parameter. We focused our attention onto the contribution of various phonon-mediated processes to spin−lattice relaxation by examining the temperature dependence of T_1. Low-energy vibrational modes dissipate the energy released during electronic spin−lattice relaxation. Two such low-energy phonon-mediated processes

DOI: 10.1021/jacs.6b08467
J. Am. Chem. Soc. 2016, 138, 14678−14685

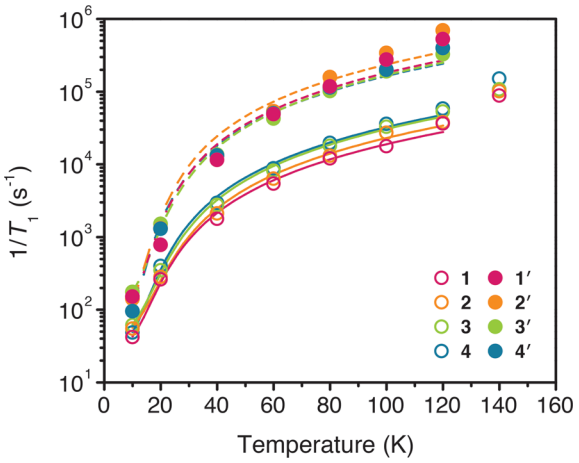

Figure 4. Spin−lattice relaxation rates ($1/T_1$) of **1**−**4** (open circles) as a function of temperature in 1:1 DMF:Tol. Closed circles correspond to the previously measured series **1′**−**4′**. The magnitude of T_1 for **1**−**4** is approximately half to one order of magnitude larger than those observed in **1′**−**4′** across the entire temperature range. Solid lines represent the fits to **1**−**4** from 10 to 120 K, and the dotted lines represent the fits to **1′**−**4′**. Fit parameters are reported in Table S15.

that contribute significantly to T_1 at low temperatures in a variety of vanadium(IV) complexes are the direct and Raman processes.[62,63] The first of these, the direct process, is a very low energy process that occurs via emission of a phonon corresponding to the energy of the spin-flip relaxation. It is typically dominant at temperatures below 20 K. The Raman process is a two-phonon process, analogous to the Raman scattering of light, in which the difference between the energies of the absorbed and emitted phonons is equal to the energy of the spin-flip transition. In the Raman process, the excited virtual state must correspond to an energy less than the Debye temperature, which is typically on the order of 100 K for frozen solvent glasses; it is therefore typically dominant at <100 K in these systems.[62,63]

Fitting of the temperature dependence of T_1 confirms that the Raman process in **1′**−**4′** possesses a coefficient approximately 10-fold higher than that of **1**−**4** (see Table S15), and is therefore responsible for the majority of the difference in T_1 between the two series. Further, fitting the Debye temperature yields similar values of 112−127 K between the two series, which confirms that the Debye temperature does not contribute to the difference in T_1.[62] As the contribution of the Raman process to T_1 is governed by low-frequency vibrational modes involving the spin center,[61,64] the differing Raman coefficients indicate that a difference in the vibrational environment around the vanadium center is the underlying cause of the T_1 disparity.

Supporting our hypothesis, multiple studies note that measuring the same species in increasingly polar solvents yields increasing values of T_1.[61,64] Such results suggest that the local molecular environment may be more important in determining the relevant vibrational environment than specific bonds within the complex. Specifically, previous T_1 studies of **1′**−**4′** note that as the solvent polarity increases from DMF:Tol to butyronitrile:DMF, T_1 of all the complexes increases at least 2-fold.[32] To test the impact of solvent polarity in this vanadyl system, we conducted a variable-temperature T_1 solvent dependence study with complex **4** in 4:1 DMF:dimethyl sulfoxide (DMSO), 1:1 dichloromethane (DCM):butyronitrile (PrCN), and 1:1 2-methyltetrahydrofuran (MTHF):Tol (Table S9, Figure S3). Fitting the temperature dependence of T_1 yielded coefficients for the Raman process that increased by a factor of 2 from the most polar solvent, DMF:DMSO, to the least polar, MTHF:Tol (see Table S16). Based on these results, we propose that vanadyl complexes, which are distinctly more polar than their VS_6 analogues, interact more strongly with the solvent matrix. In addition, the presence of the bare oxygen atom may enable stronger interactions with surrounding DMF molecules. We argue that this strong vibrational coupling serves to directly rigidify the spin center in **1**−**4** with respect to its local environment and suppresses the low-energy molecular vibrations that diminish T_1. We therefore propose the design principle that polarity of the vanadyl complex enables the longer T_1 observed in **1**−**4** over **1′**−**4′**.

There are suitable alternate explanations, which we discount for the following reasons. In principle, differences in electron delocalization between the two series may explain the increase in T_1 on moving from VS_6 to vanadyl. Here, such differences could lead to dissimilar interactions with the solvent matrix. As noted above, however, if this were a contributing factor, one would expect a significant difference between the T_1 value of **1′** and those of **2′**−**4′**—a difference that is not observed. Thus, these data suggest that the range of electron delocalization onto the ligands observed in **1**−**4** and **1′**−**4′** does not have a significant effect on the spin−lattice relaxation time.

Another well-documented contributor to spin−lattice relaxation rate is spin−orbit coupling, which couples lattice vibrations (phonons) to the electron spin.[19] Indeed, increasing spin−orbit coupling, which can be parametrized by *g*-anisotropy ($\Delta g = |g_{\parallel} - g_{\perp}|$), directly correlates with decreasing T_1 values.[61,63,65] While a recent study suggested the difference in T_1 between VS_6 and vanadyl species may be attributed to the differences in spin−orbit coupling,[28] our investigation suggests the difference in *g*-anisotropy across the series of eight molecules is insufficient to generate this disparity in T_1. Analysis of Δg in both sets of molecules yielded values that span from 0.015 to 0.019 for **1**−**4** (see Tables S5 and S6) and from 0.019 to 0.031 for **1′**−**4′**. Between pairs of analogous vanadyl and VS_6 complexes (e.g., **1** vs **1′**, **2** vs **2′**, etc.), the differences in *g*-anisotropy ($|\Delta g_{\text{vanadyl}} - \Delta g_{VS_6}|$) spanned 0.003−0.013. Differences in *g*-anisotropy of a similar magnitude in vanadium(IV) complexes in a previous study correlated with a factor of 2−4 variation in T_1, and were not determined to be a major contributor to spin−lattice relaxation.[62] Here, we observe a much larger factor of 3−10 difference in T_1 between analogous members of the two series. Further, we note a lack of discernible trend in T_1 from variation of Δg within each series. Thus, on the basis of these data, we conclude that the observed differences in spin−orbit coupling are not the origin of the large difference in T_1 between the series.

Another possibility we considered is whether changes in T_1 can be attributed to a specific local vibrational mode. Indeed, when we initiated this investigation we believed that could be a source of decoherence, and performed spectroscopic measurements to search for such a mode. Our fits of the EPR data to a Raman process suggest that the energy scale of the identifiable local modes such as the vanadium-oxo stretch is too high to influence the observed T_1 disparity. The phonon modes involved in the Raman process possess energies less than the Debye temperature, and for our systems the maximum phonon energies are approximately 83 cm^{-1}. As noted previously, the

DOI: 10.1021/jacs.6b08467
J. Am. Chem. Soc. 2016, 138, 14678−14685

stretching modes associated with a vanadium-oxo are ~980 cm^{-1}, whereas those of V—S are approximately 400 cm^{-1}.[44,52,54] The energies of these stretching modes far exceed the range expected for the Raman process in the temperature range studied, and are not expected to contribute significantly to T_1 relaxation. Based on these observations, we conclude that although vibrations involving atoms of the first coordination sphere are likely involved in the collective modes that influence T_1 at these temperatures, it is unlikely that the energies of the specific bond stretching modes are the root cause of the observed T_1 difference between the two series. While a previous study cited these bond stretching frequencies as the source of T_1 differences between vanadyl and VS_6 complexes in crystalline matrices, we suggest our proposed local environment rigidity concept is also applicable to these systems.[28] The compact packing of the vandal complex, which results in O—H dipole interactions with the nearby cations, may engender higher energy phonon modes that do not participate in spin–lattice relaxation, thereby lengthening T_1 in vanadyl complexes.

Following the creation of a new design principle for long T_1 values in these vanadyl species, we proceeded to investigate the lifetimes of the spin superposition states (T_2). To obtain T_2 values, Hahn echo decay curves were collected at the central EPR resonance of 0.5 mM solutions of **1**–**4** in both 1:1 DMF:Tol and 1:1 DMF-d_7:Tol-d_8 from 10 to 140 K. Coherence times were extracted from these data by fitting the decay curves with stretched or biexponential functions, and the T_2 values are plotted alongside those of **1′**–**4′** in Figure 5.

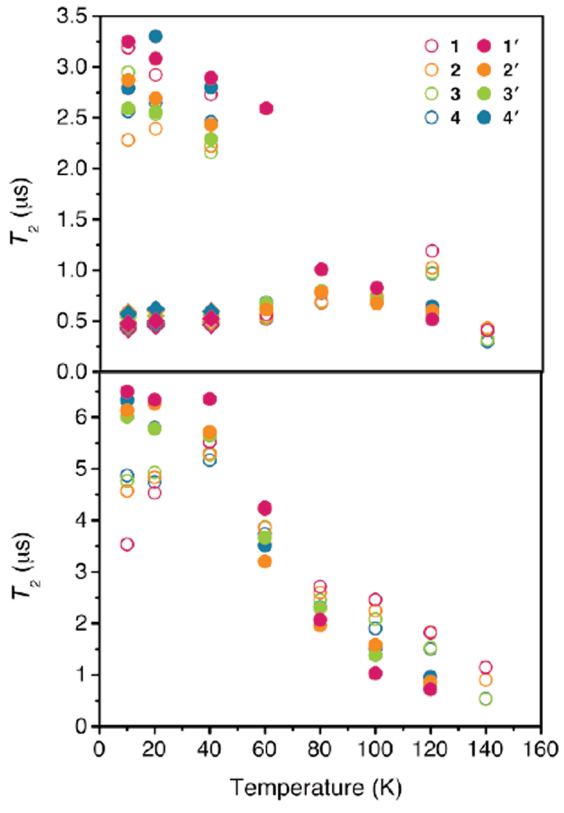

Figure 5. Decoherence times (T_2) as a function of temperature in 1:1 DMF:Tol (top) and 1:1 DMF-d_7:Tol-d_8 (bottom). Open symbols correspond to **1**–**4**, while the closed symbols correspond to **1′**–**4′**. Diamond symbols correspond to the fast process in the biexponential fits.

In 1:1 DMF:Tol, the coherence times of **1**–**4** are nearly identical to those of **1′**–**4′**, reaching 3.2(2) μs at the lowest temperatures. We note that **1**–**4** exhibit distinctly biexponential decay curves in DMF:Tol below 40 K, similar to **1′**–**4′**. This implies the presence of two separate populations of spins, each subject to a distinct set of decay processes. As the temperature increases, the curve shape is better fit by a stretched exponential function, and there is a concerted drop-off in T_2 at 60 K. A notable difference between the two series occurs at 120 K, where the T_2 values of **1**–**4** rise while those of **1′**–**4′** decrease.

In the deuterated solvent mixture, a difference is observed between the two series below 40 K, with **1**–**4** displaying T_2 parameters from 3.5(2) to 4.87(8) μs at 10 K, between 1.2 and 3.0 μs shorter than the corresponding species in **1′**–**4′**. Furthermore, the biexponential behavior is notably absent for both series, as the echo decays are well fit to a stretched exponential function. Above 40 K, both series demonstrate similar temperature dependences in T_2, and exhibit the same concerted drop in T_2 at 60 K observed in the protiated solvent matrix.

Inspection of these data reveals crucial insight into factors governing the relative qubit performance of these two sets of compounds. Specifically, the role of methyl rotation on the rate of decoherence may be an important factor to account for in this system. At low temperature, the biexponential behavior for both **1**–**4** and **1′**–**4′** is absent in the deuterated solvent, suggesting contributions from methyl group tunneling rotation at low temperatures in 1:1 DMF:Tol (see Supporting Information for details). As the temperature increases, the concerted drop in T_2 at 60 K in both solvent systems can be attributed to increased decoherence from the onset of classical methyl rotation occurring on the time scale of the T_2 measurement.[66] Finally, as the temperature is further increased to 120 K, the increase in T_2 of **1**–**4** is can be ascribed to the methyl rotation time scale becoming much shorter than the experimental time scale. This phenomenon causes coupling to individual protons on the methyl group to be averaged out and their contribution to decoherence to diminish.[19,61] Such behavior would also likely occur in **1′**–**4′** were it not for the significantly lower T_1; at 120 K, T_2 for the VS_6 series is virtually identical to that of T_1, meaning that T_2 is T_1-limited. T_1 limitation also occurs in the vanadyl species; however, it occurs at a temperature that is ~20 K higher, causing T_2 to drop significantly between 120 and 140 K.

Though methyl rotation explains the difference in behavior between solvent systems, it does not address the low-temperature discrepancy in T_2 between **1**–**4** and **1′**–**4′**. To explain this difference, the concept of a nuclear spin diffusion barrier must be invoked (Figure 6). Nuclear spins within a given distance of an electronic spin center exhibit dipolar coupling to the electron spin. When strong enough, this coupling impedes the rapid spin flips that induce decoherence. The volume in which dipolar coupling enables the slowing of spin flips is defined by the so-called nuclear spin diffusion barrier. The radius of this barrier around an electronic spin is typically estimated as 3–10 Å in protiated environments.[19,66] Transitioning from a protiated to a deuterated environment contracts the diffusion barrier around an electronic spin. The smaller deuterium magnetic moment engenders weaker dipolar coupling with the electronic spin, thereby diminishing the spatial extent to which spin flips are suppressed and hence the radius of the diffusion barrier.

DOI: 10.1021/jacs.6b08467
J. Am. Chem. Soc. 2016, 138, 14678–14685

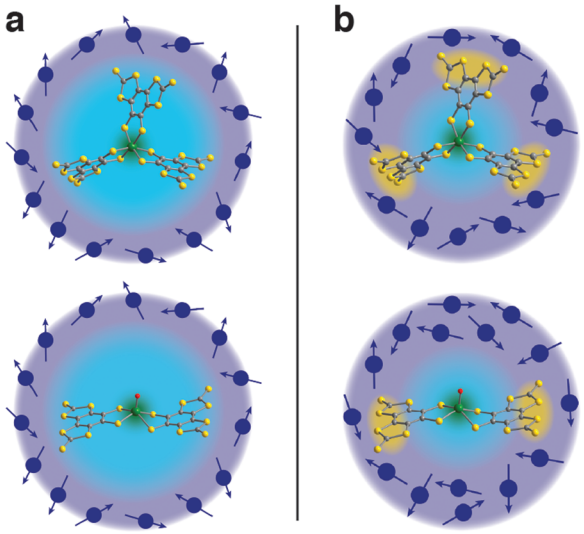

Figure 6. Proposed model of the spin diffusion barrier of **1** and **1′** in (a) 1:1 DMF:Tol and (b) 1:1 DMF-d_7:Tol-d_8. The light blue region depicts the extent of the spin diffusion barrier, while the light purple region indicates the region containing nuclear spins that contribute to decoherence. The yellow regions portray regions of space where the nuclear spin-free ligand displaces decoherence-active solvent spins. In the deuterated solvent, the replacement of a $C_8S_8^{2-}$ ligand with an oxo results in more solvent deuterons in close proximity to the electron spin that contribute to decoherence.

We therefore propose that in a protiated environment, all of the ligands are located entirely within the barrier radius (Figure 6a). Hence, replacing one ligand with an oxo does not alter the quantity of nuclear spins contributing to decoherence. However, in a deuterated environment, the barrier radius shrinks, and the ligands protrude into the decoherence-active portion of the spin bath (Figure 6b). Removing one ligand in a deuterated environment causes decoherence-active solvent deuterons to replace the nuclear spin-free ligand; these contribute to decoherence, resulting in a shorter T_2. Such a model implies that the greatest difference in T_2 between analogous members of the two series should be observed between the two species with the largest ligand, **1** and **1′**, which is indeed consistent with our results. Thus, while the oxo bond may improve molecular polarity and consequently augment T_1, the absence of the third nuclear spin-free ligand is detrimental to T_2. The use of multiple bulky, nuclear spin-free ligands is therefore established as a novel design parameter for enhancing T_2 in molecular qubits.

The foregoing results illustrate the impact of ligand field and electronic structure considerations on the performance of two analogous series of vanadium-based complexes as electronic spin-based qubits. The significant enhancement of T_2 observed in SO_2 vs deuterated solvents highlights the criticality of a nuclear spin-free environment, and demonstrates the utility of SO_2 as a nuclear spin-free solvent for future studies. Importantly, the realization of long T_2 values here highlights the promise of obtaining exceptionally long T_2 parameters in species that may readily assemble on surfaces. Our systematic study of **1**−**4** and **1′**−**4′** critically emphasizes the role of solute−solvent interactions in T_1, and suggests the polarity of a complex as an important design parameter. This is a novel design parameter for transition metal-based molecular qubits, and may lead to new directions in qubit synthesis, wherein alternative ligand sets to nonpolar carbon−sulfide structures are favored. Importantly, this work reinforces the importance of the spin diffusion barrier in determining T_2, meriting future studies on the exact extent of the barrier in vanadium-based qubits. Questions remain whether these same models, which arise from solution measurements, hold true for molecules appended to surfaces. Future studies will indeed be required to answer such questions.

■ ASSOCIATED CONTENT

Supporting Information

The Supporting Information is available free of charge on the ACS Publications website at DOI: 10.1021/jacs.6b08467.

Full experimental and crystallographic details; additional spectroscopic characterization data; Figures S1−S12 and Tables S1−S16 (PDF)

X-ray crystallographic data for **1** (CIF)

X-ray crystallographic data for **2** (CIF)

X-ray crystallographic data for **3** (CIF)

X-ray crystallographic data for **4** (CIF)

■ AUTHOR INFORMATION

Corresponding Author

*danna.freedman@northwestern.edu

Notes

The authors declare no competing financial interest.

■ ACKNOWLEDGMENTS

We thank M. S. Fataftah and M. L. Kelty for experimental assistance, and C. Stern for helpful discussions. We acknowledge support from Northwestern University, the State of Illinois, and the National Science Foundation for CAREER Award No. CHE-1455017 (C.-J.Y., M.J.G., J.M.Z., and D.E.F.) and Award No. CHE-1565925 (M.R.W.). M.J.G. acknowledges an NSF GRFP fellowship (DGE-1324585). This material is based upon work supported by the U.S. Department of Energy, Office of Science, Office of Basic Energy Sciences, Division of Chemical Sciences, Geosciences, and Biosciences, under Contract DE-AC02-06CH11357 at Argonne National Laboratory (J.N. and O.G.P.).

■ REFERENCES

(1) Feynman, R. P. *Int. J. Theor. Phys.* **1982**, *21*, 467−488.
(2) Lloyd, S. *Science* **1996**, *273*, 1073−1078.
(3) Aspuru-Guzik, A.; Dutoi, A. D.; Love, P. J.; Head-Gordon, M. *Science* **1996**, *273*, 1073−1078.
(4) Lambert, N.; Chen, Y.-N.; Cheng, Y.-C.; Li, C.-M.; Chen, G.-Y.; Nori, F. *Nat. Phys.* **2012**, *9*, 10−18.
(5) Nielsen, M. A.; Chuang, I. L. *Quantum Information and Quantum Computation*, 10th anniversary ed.; Cambridge University Press: Cambridge, 2000.
(6) Leuenberger, M. N.; Loss, D. *Nature* **2001**, *410*, 789−793.
(7) Aromí, G.; Aguilà, D.; Gamez, P.; Luis, F.; Roubeau, O. *Chem. Soc. Rev.* **2012**, *41*, 537−546.
(8) Troiani, F.; Affronte, M. *Chem. Soc. Rev.* **2011**, *40*, 3119−3129.
(9) Ardavan, A.; Blundell, S. J. *J. Mater. Chem.* **2009**, *19*, 1754−1760.
(10) Sato, K.; Nakazawa, S.; Rahimi, R.; Ise, T.; Nishida, S.; Yoshino, T.; Mori, N.; Toyota, K.; Shiomi, D.; Yakiyama, Y.; Morita, Y.; Kitagawa, M.; Nakasuji, K.; Nakahara, M.; Hara, H.; Carl, P.; Höfer, P.; Takui, T. *J. Mater. Chem.* **2009**, *19*, 3739−3754.
(11) Stamp, P. C. E.; Gaita-Ariño, A. *J. Mater. Chem.* **2009**, *19*, 1718−1730.
(12) Timco, G. A.; Carretta, S.; Troiani, F.; Tuna, F.; Pritchard, R. J.; Muryn, C. A.; McInnes, E. J. L.; Ghirri, A.; Candini, A.; Santini, P.;

DOI: 10.1021/jacs.6b08467
J. Am. Chem. Soc. 2016, 138, 14678−14685

Amoretti, G.; Affronte, M.; Winpenny, R. E. P. *Nat. Nanotechnol.* **2009**, *4*, 173−178.
(13) Ferrando-Soria, J.; Moreno Pineda, E.; Chiesa, A.; Fernandez, A.; Magee, S. A.; Carretta, S.; Santini, P.; Vitorica-Yrezabal, I. J.; Tuna, F.; Timco, G. A.; McInnes, E. J. L.; Winpenny, R. E. P. *Nat. Commun.* **2016**, *7*, 11377.
(14) Hill, S.; Edwards, R. S.; Aliaga-Alcalde, N.; Christou, G. *Science* **2003**, *302*, 1015−1018.
(15) Troiani, F.; Affronte, M.; Carretta, S.; Santini, P.; Amoretti, G. *Phys. Rev. Lett.* **2005**, *94*, 190501.
(16) Fataftah, M. S.; Zadrozny, J. M.; Coste, S. C.; Graham, M. J.; Rogers, D. M.; Freedman, D. E. *J. Am. Chem. Soc.* **2016**, *138*, 1344−1348.
(17) Zadrozny, J. M.; Niklas, J.; Poluektov, O. G.; Freedman, D. E. *J. Am. Chem. Soc.* **2014**, *136*, 15841−15844.
(18) Ghirri, A.; Chiesa, A.; Carretta, S.; Troiani, F.; van Tol, J.; Hill, S.; Vitorica-Yrezabal, I.; Timco, G. A.; Winpenny, R. E. P.; Affronte, M. *J. Phys. Chem. Lett.* **2015**, *6*, 5062−5066.
(19) Eaton, S. S.; Eaton, G. R. Distance Measurements in Biological Systems by EPR. In *Biological Magnetic Resonance*; Berliner, L. J., Eaton, S. S.; Eaton, G. R., Eds.; Kluwer Academic/Plenum Publishers: New York, 2000; Vol. *19*, pp 29−154.
(20) Nellutla, S.; Morley, G. W.; van Tol, J.; Pati, M.; Dalal, N. S. *Phys. Rev. B: Condens. Matter Mater. Phys.* **2008**, *78*, 054426.
(21) Graham, M. J.; Zadrozny, J. M.; Shiddiq, M.; Anderson, J. S.; Fataftah, M. S.; Hill, S.; Freedman, D. E. *J. Am. Chem. Soc.* **2014**, *136*, 7623−7626.
(22) Tesi, L.; Lucaccini, E.; Cimatti, I.; Perfetti, M.; Mannini, M.; Atzori, M.; Morra, E.; Chiesa, M.; Caneschi, A.; Sorace, L.; Sessoli, R. *Chem. Sci.* **2016**, *7*, 2074−2083.
(23) Shiddiq, M.; Komijani, D.; Duan, Y.; Gaita-Ariño, A.; Coronado, E.; Hill, S. *Nature* **2016**, *531*, 348−351.
(24) Bader, K.; Winkler, M.; van Slageren, J. *Chem. Commun.* **2016**, *52*, 3623−3626.
(25) Wedge, C. J.; Timco, G. A.; Spielberg, E. T.; George, R. E.; Tuna, F.; Rigby, S.; McInnes, E. J. L.; Winpenny, R. E. P.; Blundell, S. J.; Ardavan, A. *Phys. Rev. Lett.* **2012**, *108*, 107204.
(26) Tesi, L.; Lunghi, A.; Atzori, M.; Lucaccini, E.; Sorace, L.; Totti, F.; Sessoli, R. *Dalton Trans.* **2016**, DOI: 10.1039/C6DT02559E.
(27) Zadrozny, J. M.; Greer, S. M.; Hill, S.; Freedman, D. E. *Chem. Sci.* **2016**, *7*, 416−423.
(28) Atzori, M.; Morra, E.; Tesi, L.; Albino, A.; Chiesa, M.; Sorace, L.; Sessoli, R. *J. Am. Chem. Soc.* **2016**, *138*, 11234−11244.
(29) Hamstra, B. J.; Houseman, A. L. P.; Colpas, G. J.; Kampf, J. W.; LoBrutto, R.; Frasch, W. D.; Pecoraro, V. L. *Inorg. Chem.* **1997**, *36*, 4866−4874.
(30) Grant, C. V.; Geiser-Bush, K. M.; Cornman, C. R.; Britt, R. D. *Inorg. Chem.* **1999**, *38*, 6285−6288.
(31) Dikanov, S. A.; Samoilova, R. I.; Smieja, J. A.; Bowman, M. K. *J. Am. Chem. Soc.* **1995**, *117*, 10579−10580.
(32) Zadrozny, J. M.; Niklas, J.; Poluektov, O. G.; Freedman, D. E. *ACS Cent. Sci.* **2015**, *1*, 488−492.
(33) Atzori, M.; Tesi, L.; Morra, E.; Chiesa, M.; Sorace, L.; Sessoli, R. *J. Am. Chem. Soc.* **2016**, *138*, 2154−2157.
(34) Bertaina, S.; Gambarelli, S.; Mitra, T.; Tsukerblat, B.; Müller, A.; Barbara, B. *Nature* **2008**, *453*, 203−206.
(35) Stanwix, P. L.; Pham, L. M.; Maze, J. R.; Le Sage, D.; Yeung, T. K.; Cappellaro, P.; Hemmer, P. R.; Yacoby, A.; Lukin, M. D.; Walsworth, R. L. *Phys. Rev. B: Condens. Matter Mater. Phys.* **2010**, *82*, 201201.
(36) Takahashi, S.; Hanson, R.; van Tol, J.; Sherwin, M. S.; Awschalom, D. D. *Phys. Rev. Lett.* **2008**, *101*, 047601.
(37) Koehl, W. F.; Buckley, B. B.; Heremans, F. J.; Calusine, G.; Awschalom, D. D. *Nature* **2011**, *479*, 84−87.
(38) Bertaina, S.; Gambarelli, S.; Tkachuk, A.; Kurkin, I. N.; Malkin, B.; Stepanov, A.; Barbara, B. *Nat. Nanotechnol.* **2007**, *2*, 39−42.
(39) Zadrozny, J. M.; Graham, M. J.; Krzyaniak, M. D.; Wasielewski, M. R.; Freedman, D. E. *Chem. Commun.* **2016**, *52*, 10175−10178.
(40) Ardavan, A.; Rival, O.; Morton, J. J. L.; Blundell, S. J.; Tyryshkin, A. M.; Timco, G. A.; Winpenny, R. E. P. *Phys. Rev. Lett.* **2007**, *98*, 057201.
(41) The assignment of a $d_{x^2-y^2}$ ground state assumes a coordinate system with the *x*- and *y*-axes bisecting the angles defined by the S−V−S bonds.
(42) Kwik, W. L.; Stiefel, E. I. *Inorg. Chem.* **1973**, *12*, 2337−2342.
(43) Diamantis, A. A.; Raynor, J. B.; Rieger, P. H. *J. Chem. Soc., Dalton Trans.* **1980**, 1731−1733.
(44) Cooney, J. J. A.; Carducci, M. D.; McElhaney, A. E.; Selby, H. D.; Enemark, J. H. *Inorg. Chem.* **2002**, *41*, 7086−7093.
(45) Collison, D.; Gahan, B.; Garner, C. D.; Mabbs, F. E. *J. Chem. Soc., Dalton Trans.* **1980**, 667−674.
(46) Bryant, L. H.; Hodges, M. W.; Bryant, R. G. *Inorg. Chem.* **1999**, *38*, 1002−1005.
(47) Collison, D.; Mabbs, F. E.; Temperley, J.; Christou, G.; Huffman, J. C. *J. Chem. Soc., Dalton Trans.* **1988**, 309−314.
(48) Suzuki, T.; Ueda, K.; Kita, R.; Kokado, S.; Harigaya, K. *Polyhedron* **2005**, *24*, 2491−2496.
(49) Kirmse, R.; Dietzsch, W.; Stach, J.; Olk, R. M.; Hoyer, E. *Z. Anorg. Allg. Chem.* **1987**, *548*, 133−140.
(50) Wenzel, B.; Strauch, P. *Z. Naturforsch., B: J. Chem. Sci.* **1999**, *54*, 165−170.
(51) Olk, R. M.; Dietzsch, W.; Kirmse, R.; Stach, J.; Hoyer, E. *Inorg. Chim. Acta* **1987**, *128*, 251−259.
(52) Welch, J. H.; Bereman, R. D.; Singh, P. *Inorg. Chem.* **1988**, *27*, 2862−2868.
(53) Matsubayashi, G.; Akiba, K.; Tanaka, T. *Inorg. Chem.* **1988**, *27*, 4744−4749.
(54) Money, J. K.; Huffman, J. C.; Christou, G. *Inorg. Chem.* **1985**, *24*, 3297−3302.
(55) Henrick, K.; Raston, C. L.; White, A. H. *J. Chem. Soc., Dalton Trans.* **1976**, 26−28.
(56) Stoll, S.; Schweiger, A. *J. Magn. Reson.* **2006**, *178*, 42−55.
(57) Moro, F.; Kaminski, D.; Tuna, F.; Whitehead, G. F. S.; Timco, G. A.; Collison, D.; Winpenny, R. E. P.; Ardavan, A.; McInnes, E. J. L. *Chem. Commun.* **2014**, *50*, 91−93.
(58) Schlegel, C.; van Slageren, J.; Manoli, M.; Brechin, E. K.; Dressel, M. *Phys. Rev. Lett.* **2008**, *101*, 147203.
(59) Yang, J.; Wang, Y.; Wang, Z.; Rong, X.; Duan, C.-K.; Su, J.-H.; Du, J. *Phys. Rev. Lett.* **2012**, *108*, 230501.
(60) McGuinness, L. P.; Yan, Y.; Stacey, A.; Simpson, D. A.; Hall, L. T.; Maclaurin, D.; Prawer, S.; Mulvaney, P.; Wrachtrup, J.; Caruso, F.; Scholten, R. E.; Hollenberg, L. C. L. *Nat. Nanotechnol.* **2011**, *6*, 358−363.
(61) Du, J. L.; Eaton, G. R.; Eaton, S. S. *J. Magn. Reson., Ser. A* **1995**, *115*, 213−221.
(62) Fielding, A. J.; Back, D. B.; Engler, M.; Baruah, B.; Crans, D. C.; Eaton, G. R.; Eaton, S. S. Electron Spin Lattice Relaxation of V(IV) Complexes in Glassy Solutions between 15 and 70 K. In *Vanadium: The Versatile Metal*; Kustin, K., Pessoa, J. C., Crans, D. C., Eds.; American Chemical Society: Washington, DC, 2007; Vol. *974*, pp 364−375.
(63) Zhou, Y.; Bowler, B. E.; Eaton, G. R.; Eaton, S. S. *J. Magn. Reson.* **1999**, *139*, 165−174.
(64) Sato, H.; Kathirvelu, V.; Fielding, A.; Blinco, J. P.; Micallef, A. S.; Bottle, S. E.; Eaton, S. S.; Eaton, G. R. *Mol. Phys.* **2007**, *105*, 2137−2151.
(65) Fielding, A. J.; Fox, S.; Millhauser, G. L.; Chattopadhyay, M.; Kroneck, P. M. H.; Fritz, G.; Eaton, G. R.; Eaton, S. S. *J. Magn. Reson.* **2006**, *179*, 92−104.
(66) Zecevic, A.; Eaton, G. R.; Eaton, S. S.; Lindgren, M. *Mol. Phys.* **1998**, *95*, 1255−1263.

DOI: 10.1021/jacs.6b08467
J. Am. Chem. Soc. 2016, 138, 14678−14685